

Journal of Materials Chemistry C

Accepted Manuscript



This is an *Accepted Manuscript*, which has been through the Royal Society of Chemistry peer review process and has been accepted for publication.

Accepted Manuscripts are published online shortly after acceptance, before technical editing, formatting and proof reading. Using this free service, authors can make their results available to the community, in citable form, before we publish the edited article. We will replace this *Accepted Manuscript* with the edited and formatted *Advance Article* as soon as it is available.

You can find more information about *Accepted Manuscripts* in the [Information for Authors](#).

Please note that technical editing may introduce minor changes to the text and/or graphics, which may alter content. The journal's standard [Terms & Conditions](#) and the [Ethical guidelines](#) still apply. In no event shall the Royal Society of Chemistry be held responsible for any errors or omissions in this *Accepted Manuscript* or any consequences arising from the use of any information it contains.

Epitaxy-Driven Vertical Growth of Single-Crystalline Cobalt Nanowire Arrays by Chemical Vapor Deposition

Cite this: DOI: 10.1039/x0xx00000x

Received 00th January 2012, Accepted 00th January 2012

Si-in Kim,^a Hana Yoon,^{ab} Hyoban Lee,^a Sunghun Lee,^a Younghun Jo,^c Sungyul Lee,^d Jaebum Choo,^{*e} and Bongsoo Kim^{*a}

DOI: 10.1039/x0xx00000x

www.rsc.org/

Highly-oriented single-crystalline ferromagnetic Co nanowire (NW) arrays were synthesized on sapphire substrates *via* single-step chemical vapor deposition (CVD) method. On an *m*-cut sapphire substrate, Co NWs were vertically grown in epitaxial relationship with the substrate without using any catalysts or templates. On a *r*-cut sapphire substrate, Co NWs were horizontally grown in two perpendicular directions. Furthermore, we report that the Co NWs were transformed into Co₃O₄ nanotubes by thermal annealing in dilute O₂ condition. Such formation of hollow structures is ascribed to favored outward diffusion of Co ions. The present vertically aligned arrays of single-crystalline Co NWs could be utilized to advanced magnetic memory applications owing to their uniform orientations.

Introduction

Metal nanowires (NWs) that are ferromagnetic at room temperature have played important roles in diverse applications of nanoelectronics and nanospintronics.¹⁻⁵ In the fabrication of NW device, while the bottom-up approach is simpler in synthetic procedures as well as able to produce NWs with more diverse compositions than the top-down approach, it requires technologies to integrate as-grown materials into the desired platform.⁶ Well-ordered ferromagnetic NW arrays can be utilized for high-density magnetic information storages.^{1,4} In order to drive these ferromagnetic NWs into efficient device components, it is also critical to form single-crystalline NWs because the crystallinity of ferromagnetic NWs can significantly affect both the behavior of magnetic domain wall inside the NW and subsequent implementation of reliable device.⁷ Therefore, it is highly desirable to synthesize single-crystalline Co NWs in a specific orientation for future high-density magnetic recording devices and magnetic sensors.

So far, the most common and well-studied technique for the synthesis of Co NW is the electrodeposition method based on the template having anisotropic channels such as anodic aluminum oxide (AAO), polycarbonate, and diblock copolymer.⁸⁻¹³ However, these methods require complex multi-step template preparation as well as the post-synthesis NW purification processes. It is also rather difficult to synthesize single-crystalline NWs by these methods. Recently, Liakakos *et al.* reported direct epitaxial vertical growth of hexagonal close-packed (hcp) Co NWs on a metal film by reduction of coordination compound in solution phase,¹⁴ which was much more effective than previous methods. In these solution-based synthetic methods, vertically-grown NWs aggregate into a

bundle form as the solvent evaporated, making it rather hard to fabricate independent memory unit of individual NW.

Herein, we report epitaxial growth of Co NW arrays in vertical orientation on a sapphire substrate by a single-step chemical vapor deposition (CVD) method without using any templates. CVD method only requires proper substrates and precursors without template materials. It made possible synthesis of many useful single crystalline metal NWs including Ni, Au, Pd, and AuPd cost-effectively with simple preparation steps.^{15,16} Furthermore, He *et al.* produced ultrathin Pb NWs in the 6 nm pores of SBA-15 mesoporous silica substrates by CVD method.¹⁷ This approach provides a simple synthetic process of aligned arrays of single-crystalline Co NWs. The single-crystallinity and ferromagnetism of Co NWs were confirmed by electron diffraction and SQUID measurement, respectively. Furthermore, as-synthesized Co NWs can be transformed to Co₃O₄ nanotubes through thermal annealing in the presence of dilute O₂. It is anticipated that the aligned arrays of single-crystalline and ferromagnetic Co NWs could be quite valuable for development of advanced magnetic memory applications by integration of nanomaterials. Subsequently fabricated Co₃O₄ nanotubes can be utilized as heterogeneous catalysts, gas sensors, and electrochromatic devices.¹⁸⁻²⁰

Experimental

Synthesis of Co NWs

We synthesized Co NWs in a 1 in. diameter quartz tube using a horizontal hot-wall single/dual zone furnace (ESI, Fig. S1a). The setup was equipped with pressure and mass flow controllers. The upstream (US) zone and downstream (DS)

zone were used for vaporization of precursor and NW growth, respectively. Anhydrous CoCl_2 beads (0.05 g, 99.9% purity, Sigma-Aldrich) in an alumina boat used as Co precursors were placed at the center of the US heating zone. Prior to the start of the deposition, all Al_2O_3 substrates were cut by diamond cutter to a $5 \times 5 \text{ mm}^2$ size, cleaned with acetone in an ultrasonic bath for 10 min, and then dried with nitrogen gas. The Co NWs grew on a rectangular Al_2O_3 substrate placed on a carbon powder (99.9% purity, Alfa), which was located at $\sim 12 \text{ cm}$ downstream from the precursors. The temperatures of the US zone and DS zone were then heated at 670 and 950 $^\circ\text{C}$, respectively, for 10 min of reaction time with Ar flow at 200 sccm, while the chamber pressure was maintained at 760 Torr during the reaction. No catalyst or template were used. As-synthesized vertical Co NWs are not easily removed from substrate due to epitaxial relationship with substrate. To prepare a TEM sample, we could disperse some vertical Co NWs in ethanol by ultrasonication for tens of minutes.

Transformation from Co NWs to Co_3O_4 nanotubes

For fabrication of Co_3O_4 nanotubes, as-synthesized Co NWs grown on the Al_2O_3 substrate were placed at the center of heating zone in the same furnace system (ESI, Fig. S1b). NW crystal transformation was carried out at 250 \sim 600 $^\circ\text{C}$ under a flow rate of 250 sccm of 20 % O_2/Ar at atmospheric pressure for 10 \sim 30 min.

Characterization

XRD pattern of the specimen was recorded on a Rigaku D/max-rc (12 kW) diffractometer operated at 30 kV and 60 mA with filtered $\text{CuK}\alpha$ radiation. Field emission scanning electron microscope (FESEM) images of Co NWs were taken on a Phillips XL30S and Nova 230. Transmission electron microscope (TEM) images, high-resolution TEM (HRTEM) images, selected area electron diffraction (SAED) patterns, energy-dispersive X-ray spectrometry (EDS) and electron energy-loss spectroscopy (EELS) spectra were taken on a JEOL JEM-2100F TEM operated at 200 kV. After nanostructures were dispersed in ethanol, a drop of the solution was placed on a carbon film coated copper grid for TEM analysis. For the cross-section TEM study of Co NW and the interface between the sapphire substrate and the Co NW, a cross-section was sliced and thinned using a focused ion beam (FIB). The temperature and field dependences of the magnetization were measured by using a commercial superconducting quantum interference device (SQUID) magnetometer (Quantum Design, MPMS7).

Results and discussion

Fig. 1 shows representative scanning electron microscope (SEM) images of as-synthesized NWs in vertical orientations on a large area of substrate. The Co NW arrays were successfully synthesized on an *m*-cut ($10\bar{1}0$) sapphire substrate *via* CVD method using furnace without catalyst and template, and have diameters of 100 \sim 250 nm and lengths of several μm . Magnified 45 $^\circ$ tilted-view SEM images in Fig. 1b and inset display that the NWs have clear facets and are well-aligned on a substrate as marked by yellow dashed lines. Inset image illustrates a flat tip and rectangular cross-section of NW. Top-view SEM image of the NWs (Fig. 1c) for the same region in Fig. 1b confirms again that as-synthesized NWs have rectangular cross-sections (see red circles). Small spherical Co

particles are also synthesized on the substrate in addition to vertical Co NWs. It has been reported that the diameter of FeSi NWs could be controlled in a wide range by adjusting the amount of Si precursor.²¹ Similarly, we anticipate that the diameter of Co NWs can be controlled through the adjustment of reaction conditions such as the amount of CoCl_2 precursor as well as their temperature, and that this diameter control could play a major role in sensing based application.

XRD pattern of vertically-grown NW arrays indicates that face-centered cubic (fcc) Co with a lattice constant of 3.544 \AA (space group Fm3m, JCPDS card No. 15-0806) is the only phase presented except for sapphire substrate peaks (ESI, Fig. S2). Indeed, it is well-known that Co has two kinds of phases.²²

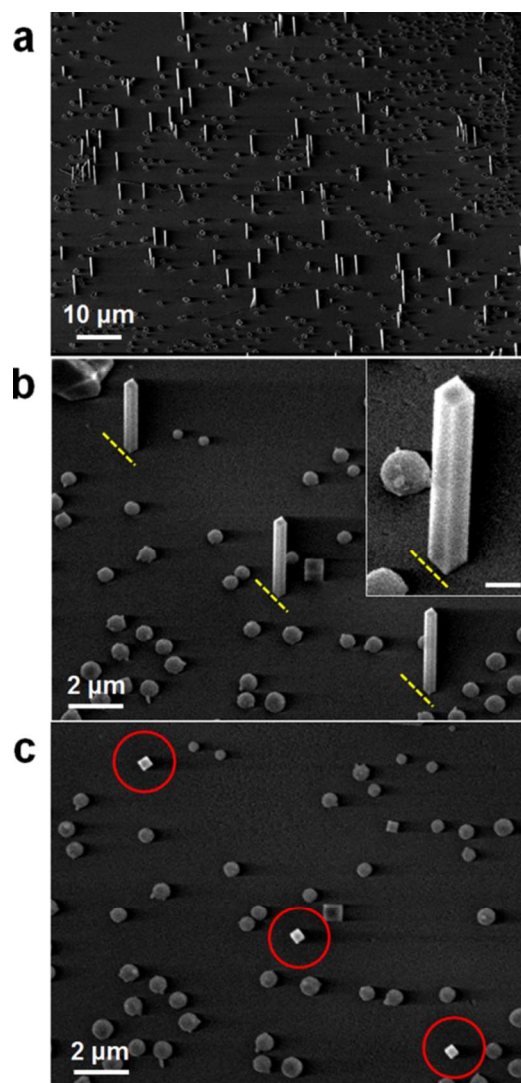


Fig. 1. SEM images of arrays of vertical Co NWs obtained by chemical vapor deposition on an *m*-cut sapphire substrate. (a) 45 $^\circ$ tilted-view of NW arrays. (b) Magnified 45 $^\circ$ tilted-view and (c) top-view images of the same region. Inset in (b) is a magnified image of a NW displaying the tip shape. Co NWs with a rectangular cross-section (red circles in (c)) were well-aligned on a substrate as marked by yellow dashed lines. Scale bar in inset of (b) is 500 nm.

While the hcp Co structure is more stable than fcc Co at room temperature, Co with fcc phase also exists at room temperature

depending on synthetic conditions since the energy difference of two structures is not quite large. Thus many Co nanostructures can have fcc structure or mixed structures of hcp and fcc at room temperature.²³

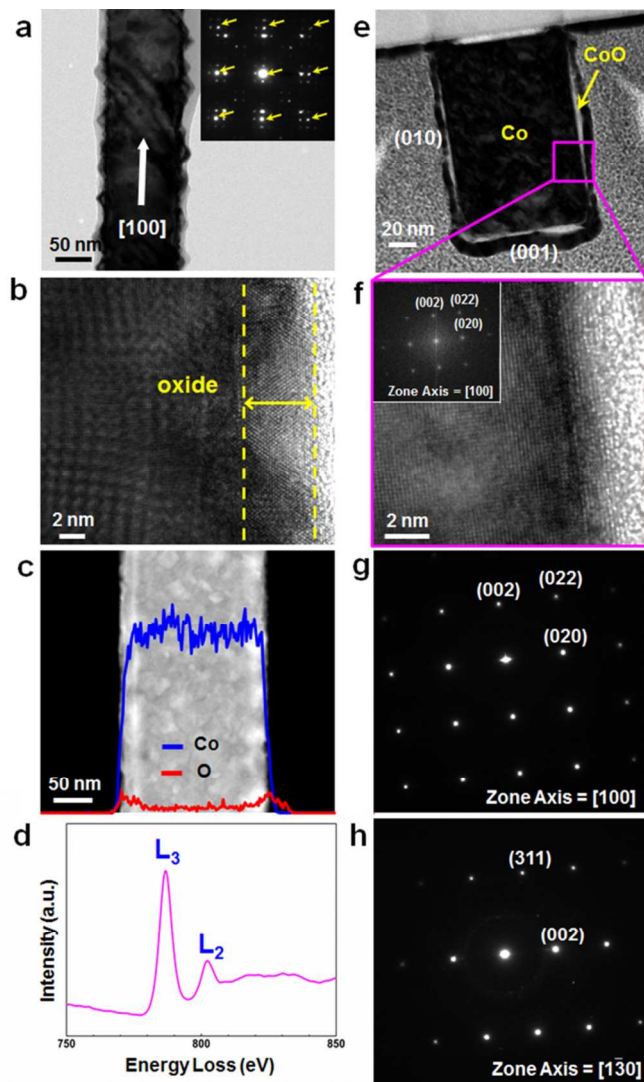


Fig. 2. TEM images of Co NWs vertically grown on *m*-cut sapphire substrates. (a) Representative TEM image and SAED pattern (inset). Analysis of the spots marked by arrows indicates that the NW has fcc Co phase with [100] growth direction. (b) HRTEM image shows that the NW is covered by a ~ 5 nm thick crystalline cobalt oxide layer (yellow dashed line). (c) EDS line profile of a Co NW. Atomic percentages of Co and O elements in the NW are shown as blue and red lines, respectively, along the short axis of the NW. (d) EELS spectrum of an oxide layer on the outer surface of a Co NW, revealing that the shell is composed of CoO. (e) Cross-sectional TEM image of a Co NW cut perpendicular to the growth direction. (f) HRTEM image of the pink square in (e) and FFT pattern (inset image). (g,h) SAED patterns of a Co NW cross-section along zone axes of [100] (g) and $[1\bar{3}0]$ (h).

TEM investigation shows that rough oxide layers are formed on the surface of as-synthesized Co NWs presumably due to immediate surface oxidation.^{24,25} Diffraction spots from the Co

single-crystal appear as multiple spots by the thin crystalline oxide layer on the NW surface (inset of Fig 2a). Analysis of the spots marked by arrows indicates that the NW has fcc Co phase with [100] growth direction. High-resolution TEM (HRTEM) image in Fig. 2b exhibits that the oxide layer is crystalline with a thickness of 5 \sim 10 nm indicated by yellow dashed lines. Nonuniform lattice fringes in the core region of the NW (Fig. 2b) are also due to the presence of a crystalline oxide layer. Energy-dispersive X-ray spectroscopy (EDS) line profile analysis shows that Co atoms are evenly distributed over the whole diameter of the NW, whereas O atoms are more highly concentrated in the outer region than the inner region of the NW (Fig. 2c). Such distribution of O atoms is consistent with the fact that as-synthesized Co NWs are covered with thin oxide layers. Cobalt oxide typically has three different compositions, CoO, Co₂O₃, and Co₃O₄, among which CoO and Co₃O₄ are more stable.²⁶ The chemical compositions of oxides in the NW surface were measured by EDS at five points on the NW surface (ESI, Fig. S3), showing that Co:O atomic ratio is close to 1:1 near the outermost surface and suggesting a structure of CoO. There might be a minor error in oxygen EDS signal due to natural oxidation of Cu grid.

Electron energy-loss spectroscopy (EELS) measurement of as-synthesized Co NWs reveals the chemical bonding state of cobalt oxide over the NW surface (Fig. 2d). L₃ and L₂ peaks detected from the first transition-series metal elements are sensitively affected by the oxidation state of metals, and we can determine the oxidation state of Co in an oxide shell by comparing the area of these two peaks. L₃ and L₂ peaks have an area of 1.94×10^6 and 6.35×10^5 , respectively, with an area ratio of 3.04. This value is closest to that of CoO among Co₃O₄ (2.43), CoO (2.90), and Co (3.77), and thus it is most likely that the chemical composition of the cobalt oxide layer is mainly CoO.²⁷ Ferromagnetic Co NWs covered with antiferromagnetic CoO layer can show exchange bias effect at interface by coupling of two materials. In this study, however, such phenomenon was not observed in hysteresis loop because the diameter of Co NW (100 \sim 250 nm) is large compared to the thickness of CoO layer (5 \sim 10 nm).

The crystallinity of Co NWs was investigated by cross-sectional TEM analysis after vertically-grown NWs were transferred onto a silicon substrate by pressing and then sliced and thinned by a focused ion beam (FIB) technique. To protect the sample from the ion beam during milling, a Pt layer was deposited on the desired region by using FIB gas injection prior to ion milling. Low-resolution TEM image in Fig. 2e shows that cross-section of the NW is a rectangle, consistent with the observation by SEM. An oxide layer is clearly observed in Fig. 2e,f. Fig. 2f is a magnified HRTEM image of the pink square region in Fig. 2e and displays uniform and clear lattice fringes of a Co NW. Fast Fourier transform (FFT) pattern (Fig. 2f inset) and SAED patterns (Fig. 2g,h), observed at different zone axes, demonstrate that the Co NWs are defect-free single-crystalline and vertically grow along the [100] direction, and the side and top facets are all {100}.

Fig. 3a shows the cross-sectional TEM image of a vertical Co NW grown on an *m*-cut sapphire substrate, cut perpendicular to the substrate along the pink dashed line (in inset). The upper part of the NW was damaged by ion milling during sample preparation. Fig. 3b is a HRTEM image of the

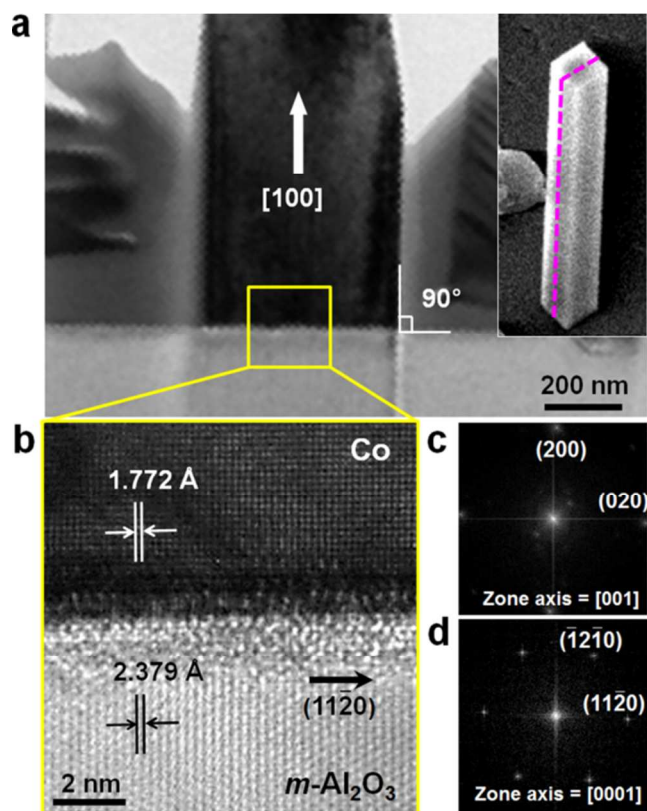


Fig. 3. (a) Cross-sectional TEM image of a vertically grown Co NW cut parallel to the growth direction (see the dashed pink line in inset). (b) HRTEM image of the interface between a NW and substrate of the yellow square in (a). (c,d) FFT patterns of the NW and substrate, respectively.

interface between the NW and substrate (see yellow square in Fig. 3a), and Fig. 3c,d show FFT patterns of the NW and substrate, respectively. Analysis of the HRTEM image and FFT patterns reveals that epitaxial relationship between the vertical Co NW and *m*-cut sapphire substrate is $(200)\text{Co} // (1\bar{1}00)\text{Al}_2\text{O}_3$. At interface, the lattice mismatch between the $\langle 020 \rangle$ direction of Co and the $\langle 11\bar{2}0 \rangle$ direction of Al_2O_3 is 24.6 % and that between the $\langle 001 \rangle$ direction of Co and the $\langle 0001 \rangle$ direction of Al_2O_3 is 17.8 %. In a domain matching epitaxy, five layers of Co are matched with three layers of Al_2O_3 along the Co $\langle 020 \rangle$ direction with only a 0.56 % mismatch, and five layers of Co are matched with four layers of Al_2O_3 along the Co $\langle 001 \rangle$ directions with 2.8 % mismatch. While the growth of Co NWs through electrodeposition using a template with anisotropic channels has been intensively studied,⁸⁻¹³ direct synthesis of ordered Co NWs on the substrate were quite rarely reported.¹⁴

To make these Co NWs more applicable to 3-dimensional magnetic memory devices, both more uniform homogeneity and higher density are required. Since the vertical NW growth propensity is mostly provided by direct impingement to the substrate from the vapor, to increase the density of vertical NWs, it is needed to increase impingement rate to the substrate from the vapor, in other words, the density of the Co atoms in the vapor. Further optimization can be achieved through control of experimental parameters, such as substrate temperature, vapor flux of Co, chamber pressure, and furnace heating rate. In addition, since it is known that Co epitaxial thin film can be grown in either fcc phase or hcp phase on a sapphire substrate

depending on the substrate temperature, we expect that hcp-structured Co NWs having a higher magnetic crystalline anisotropy could be also obtained at higher substrate temperature than currently used for the synthesis of fcc-structured Co NWs.²⁸

Interestingly, horizontal Co NWs aligned in two directions were synthesized when *r*-cut ($1\bar{1}02$)sapphire was employed as a substrate instead of *m*-cut sapphire while other experimental conditions were kept the same (ESI, Fig. S4). We found that as-synthesized horizontal Co NW has a hcp crystal structure unlike vertical Co NW. The horizontal Co NWs have a hexagonal cross-section and an oxide layer at surface, and grow along $[0001]$ direction. Furthermore, Co NWs possessing several twin planes as well as twin-free NWs were synthesized at the same time with stacking faults observed in both NWs. The two orientations of the horizontal NWs perpendicularly crossing on a *r*-cut sapphire substrate could be explained as follows. Fine lattice match is retained when Co lattice is rotated by 90° with respect to the favorable substrate lattice. It is well-known that the interfacial energy between the NW and the substrate varies depending on the crystal orientation of substrate and the atomic distribution matching, and consequently may affect growth orientation and crystal structure of the Co NWs.²⁹ A detailed analysis of the mechanism is currently in progress.

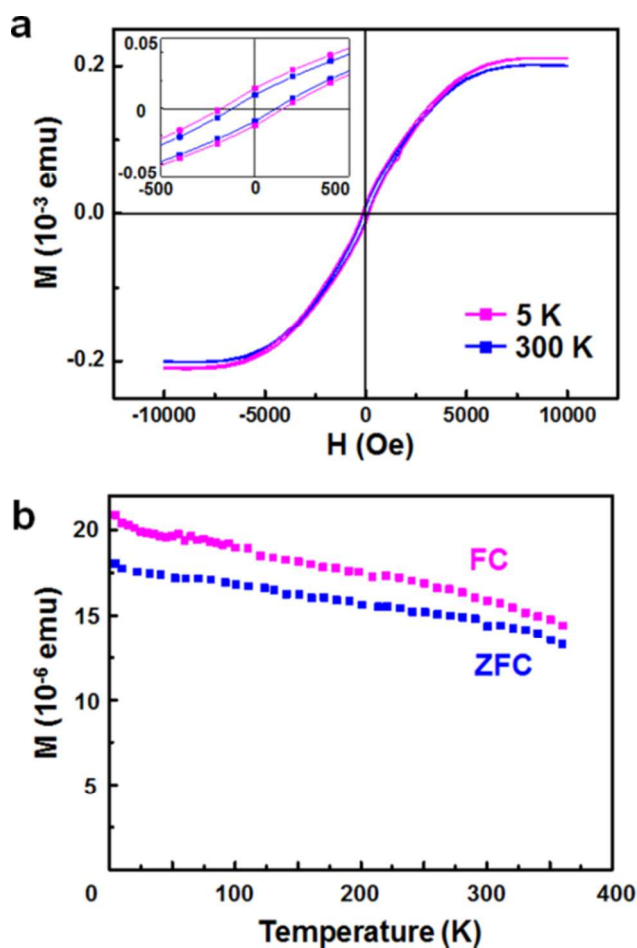


Fig. 4. Magnetic properties of Co NW arrays. (a) Plot of M as a function of H at 5 and 300 K, respectively. Inset shows loops on an enlarged scale. (b) Plot of M as a function of T at an

applied field of 500 Oe. Pink and blue squares represent the FC and ZFC data, respectively.

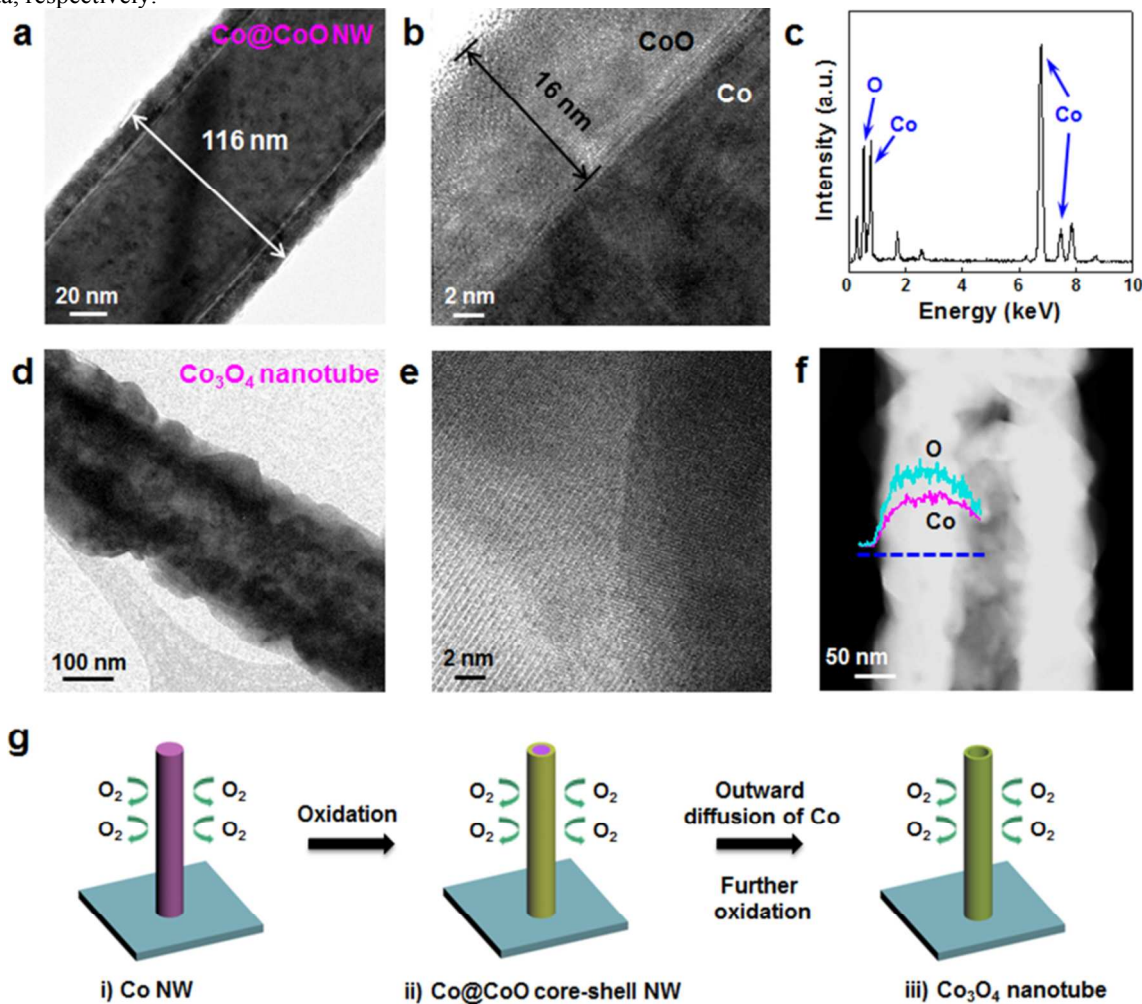


Fig. 5. (a,b) TEM images of Co@CoO core-shell NW structure synthesized at 250 °C for 30 min. (c) EDS spectrum of the shell part showing that atomic composition ratio is Co:O ~ 1:1. (d,e) TEM images of a Co₃O₄ nanotube obtained at 600 °C for 10 min. (f) STEM image and EDS line profiles along the blue dashed line, indicating Co₃O₄ composition of nanotube. (g) A schematics of the formation process of a Co₃O₄ nanotube from Co NWs during thermal annealing in a dilute O₂ condition.

Magnetic properties of vertical Co NW arrays on a sapphire substrate were examined by superconducting quantum interference device (SQUID) magnetometer. Fig. 4a shows magnetic field-dependent magnetization (M - H) curves measured at 5 and 300 K. The two M - H curves exhibit the hysteresis loop with a coercive field (H_C) of approximately 180 and 120 Oe at 5 and 300 K, respectively. The temperature-dependent magnetization (M - T) curves measured after field cooling (FC) and zero-field cooling (ZFC) under 500 Oe magnetic field are indicated in Fig. 4b. The M - T curves obtained in a temperature range from 5 to 370 K show nonzero magnetization upto room temperature in both FC and ZFC measurements. The hysteresis loop and M - T curves reveal that as-synthesized Co NWs are ferromagnetic at room temperature, which is consistent with T_C reported in bulk Co (~1388 K).³⁰ Co NWs were transformed to Co₃O₄ nanotubes by thermal annealing at 250 ~ 600 °C in 20% O₂ condition for 10 ~ 30 min. TEM results for the nanostructures obtained from reaction at 250 °C for 30 min are shown in Fig. 5a-c. While the oxide layer thickness of as-synthesized Co NWs in Fig. 1 was about 5 nm,

that of thermally oxidized NWs increased to ~ 16 nm (see the low- and high-resolution TEM images in Fig. 5a,b). The EDS spectrum (Fig. 5c) of a shell region of NW in Fig. 5b reveals that the Co:O atomic ratio is 47.3:52.8%, close to 1:1. Other peaks were attributed to Si, Cu and C from the EDS detector and TEM grid. When we increase the annealing temperature to 400 °C, oxide shell thickness further increased to ~50 nm after 10 min reaction time (ESI, Fig. S5). When the Co NWs were annealed at 600 °C for 10 min, they were converted to nanotubes (Fig. 5d-f). HRTEM image in Fig. 5e indicates that nanotube is poly-crystalline, consisting of multiply crystalline layers. Clear contrast of scanning TEM (STEM) image (Fig. 5f) demonstrates again the nanotube morphology, in which the inside is empty along the longitudinal direction. TEM-EDS line profile analysis found that atomic composition of this nanotube is Co:O=36.7:63.2. Because stable compounds of cobalt oxide are CoO and Co₃O₄, it is likely that the nanotubes have crystal structures of Co₃O₄. EDS result (Fig. 5f) indicates that Co and O elements as marked by pink and cyan lines, respectively,

have constant Co:O ratio and the nanostructure has a hollow structure.

Transformation of Co NWs to Co₃O₄ nanotubes, inferred from the TEM results, occurred by thermal annealing process following the scheme in Fig. 5g. Firstly, Co is gradually oxidized into CoO from the surface of NW by heating in dilute O₂ condition at an early stage of annealing, forming a Co@CoO core-shell NW with an oxide layer of tens of nanometer (Fig. 5a and Fig. S5).^{31,32} The formation of cobalt oxide nanotube can be explained by the nanoscale Kirkendall effect, which is attributed to difference in diffusion rates between the cation and anion.³³ Since the outward diffusion of Co is much faster than inward diffusion of O in the oxide layer, a tendency to form interior nanocavities is incurred at the interface of Co/oxide.³⁴ CoO is finally further oxidized to Co₃O₄. Such oxidation process of Co $\xrightarrow{\text{O}_2(\text{gas})}$ CoO $\xrightarrow{\text{O}_2(\text{gas})}$ Co₃O₄ has been well observed in thin Co foil and Co nanoparticles.^{31,32}

Conclusions

We reported for the first time the epitaxial growth of single-crystalline Co NWs individually aligned in vertical direction on *m*-cut sapphire substrates *via* rapid and versatile CVD method without employing any catalysts or templates. Horizontal Co NWs are grown on *r*-cut substrates. Furthermore, we demonstrated that Co₃O₄ nanotubes could be readily fabricated by thermal annealing of Co NWs *via* CoO as an intermediate material in dilute O₂ condition. It is anticipated that well-aligned single-crystalline Co NW arrays can be utilized as valuable materials including development of advanced magnetic memory applications. Additionally, Co₃O₄ nanotubes are potentially applicable to catalyst and sensing devices.

Acknowledgements

J.C. and B.K. acknowledge support by Korean Health Technology R&D Project (A121983), Ministry of Health & Welfare, Korea. TEM analysis was performed at the KBSI in Daejeon.

Notes and references

^a Department of Chemistry, KAIST, Daejeon 305-701, Korea. E-mail: bongsoo@kaist.ac.kr; Fax: +82 42-350-2810.

^b Energy Storage Department, KIER, Daejeon 305-343, Korea.

^c Nano Materials Research Team, KBSI, Daejeon 305-333, Korea.

^d Department of Applied Chemistry, Kyung Hee University, Kyungki 446-701, Korea.

^e Department of Bionano Engineering, Hanyang University, Ansan, 426-791, Korea. E-mail: jbchoo@hanyang.ac.kr; Fax: +82 31-436-8188.

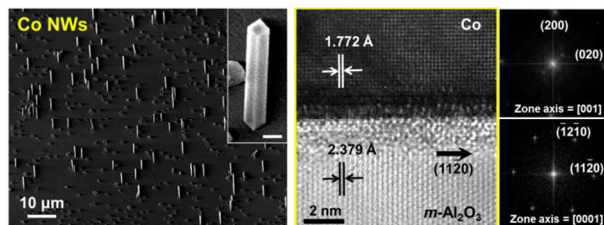
Electronic Supplementary Information (ESI) available: Experimental setup (S1). XRD pattern of Co NW arrays (S2). Chemical composition of cobalt oxide in NW surface (S3). Horizontal Co NWs grown on a *r*-cut sapphire substrate (S4). Co@CoO NW obtained by thermal annealing at 400 °C (S5). See DOI: 10.1039/b000000x/

1 X. Kou, X. Fan, R. K. Dumas, Q. Lu, Y. Zhang, H. Zhu, X. Zhang, K. Liu, J. Q. Xiao, Memory Effect in Magnetic Nanowire Arrays, *Adv. Mater.*, 2011, **23**, 1393.

- 2 H. -T. Huang, T. -R. Ger, Y. -H. Lin, Z. -H. Wei, Single Cell Detection using a Magnetic Zigzag Nanowire Biosensor, *Lab Chip*, 2013, **13**, 3098.
- 3 W. Gao, S. Sattayasamitsathit, K. M. Manesh, D. Weihs, J. Wang, Magnetically Powered Flexible Metal Nanowire Motors, *J. Am. Chem. Soc.*, 2010, **132**, 14403.
- 4 S. S. P. Parkin, M. Hayashi, L. Thomas, Magnetic Domain-Wall Racetrack Memory, *Science*, 2008, **320**, 190.
- 5 M. M. Maqableh, X. Huang, S. -Y. Sung, K. S. M. Reddy, G. Norby, R. H. Victora, B. J. H. Stadler, Low-Resistivity 10 nm Diameter Magnetic Sensors, *Nano Lett.*, 2012, **12**, 3102.
- 6 M. C. P. Wang, B. D. Gates, Directed Assembly of Nanowires, *Materialstoday*, 2009, **12**, 34.
- 7 F. Garcia-Sanchez, H. Szabolcs, A. P. Mihai, L. Vila, A. Marty, A. M. Attane, J. -C. Toussaint, L. D. Buda-Prejbeanu, Effect of Crystalline Defects on Domain Wall Motion under Field and Current in Nanowires with Perpendicular Magnetization, *Phys. Rev. B*, 2010, **81**, 134408.
- 8 X. Huang, L. Li, X. Luo, X. Zhu, G. Li, Orientation-Controlled Synthesis and Ferromagnetism of Single Crystalline Co Nanowire Arrays, *J. Phys. Chem. C*, 2008, **112**, 1468.
- 9 P. Yang, M. An, C. Su, F. Wang, Fabrication of Cobalt Nanowires from Mixture of 1-Ethyl-3-Methylimidazolium Chloride Ionic Liquid and Ethylene Glycol using Porous Anodic Alumina Template, *Electrochimica Acta*, 2008, **54**, 763.
- 10 L. Cattaneo, S. Franz, F. Albertini, P. Ranzieri, A. Vincenzo, M. Bestetti, P. L. Cavallotti, Electrodeposition of Hexagonal Co Nanowires with Large Magnetocrystalline Anisotropy, *Electrochimica Acta*, 2012, **85**, 57.
- 11 J. Qin, J. Noguez, M. Mikhaylova, A. Roig, J. S. Munoz, M. Muhammed, Differences in the Magnetic Properties of Co, Fe, and Ni 250-300 nm Wide Nanowires Electrodeposited in Amorphous Anodized Alumina Templates, *Chem. Mater.*, 2005, **17**, 1829.
- 12 L. Vila, P. Vincent, L. D. Pra, G. Pirio, E. Minoux, L. Gangloff, S. Demoustier-Champagne, N. Sarazin, E. Ferain, R. Legras, L. Piroux, P. Legagneux, Growth and Field-Emission Properties of Vertically Aligned Cobalt Nanowire Arrays, *Nano Lett.*, 2004, **4**, 521.
- 13 T. Thurn-Albrecht, J. Schotter, G. A. Kastle, N. Emlay, T. Shibauchi, L. Krusin-Elbaum, K. Guarini, C. T. Black, M. T. Tuominen, T. P. Russell, Ultrahigh-Density Nanowire Arrays Grown in Self-Assembled Diblock Copolymer Templates, *Science*, 2000, **290**, 2126.
- 14 N. Liakakos, T. Blon, C. Achkar, V. Vilar, B. Cormary, R. P. Tan, O. Benamara, G. Chaboussant, F. Ott, B. Warot-Fonrose, E. Snoeck, B. Chaudret, K. Soulantica, M. Respaud, Solution Epitaxial Growth of Cobalt Nanowires on Crystalline Substrates for Data Storage Densities beyond 1Tbit/in², *Nano Lett.*, 2014, **14**, 3481.
- 15 K. T. Chan, J. J. Kan, C. Doran, L. Ouyang, D. J. Smith, E. E. Fullerton, Oriented Growth of Single-Crystal Ni Nanowires onto Amorphous SiO₂, *Nano Lett.*, 2010, **10**, 5070.
- 16 Y. Yoo, K. Seo, S. Han, K. S. K. Varadwaj, H. Kim, J. Ryu, H. Lee, J. Ahn, H. Ihee, B. Kim, Steering Epitaxial Alignment of Au, Pd, and AuPd Nanowire Arrays by Atom Flux Change, *Nano Lett.*, 2010, **10**, 432.
- 17 M. He, C. H. Wong, P. L. Tse, Y. Zheng, H. Zhang, F. L. Y. Lam, P. Sheng, X. Hu, R. Lortz, "Giant" Enhancement of the Upper Critical

- Field and Fluctuations above the Bulk T_c in Superconducting Ultrathin Lead Nanowire Arrays, *ACS Nano*, 2013, **7**, 4187.
- 18 Y. Liang, Y. Li, H. Wang, J. Zhou, J. Wang, T. Regier, H. Dai, Co_3O_4 Nanocrystals on Graphene as a Synergistic Catalyst for Oxygen Reduction Reaction, *Nat. Mater.*, 2011, **10**, 780.
- 19 H. Nguyen, S. A. El-Safty, Meso- and Macroporous Co_3O_4 Nanorods for Effective VOC Gas Sensors, *J. Phys. Chem. C*, 2011, **115**, 8466.
- 20 X. H. Xia, J. P. Tu, J. Zhang, X. H. Huang, X. L. Wang, X. B. Zhao, Improved Electrochromic Performance of Hierarchically Porous Co_3O_4 Array Film through Self-Assembled Colloidal Crystal Template, *Electrochimica Acta*, 2010, **55**, 989.
- 21 S. Kim, H. Yoon, K. Seo, Y. Yoo, S. Lee, B. Kim, Truncated Tetrahedron Seed Crystals Initiating Stereoaligned Growth of FeSi Nanowires, *ACS Nano*, 2012, **6**, 8652.
- 22 X. W. Wang, G. T. Fei, B. Wu, L. Chen, Z. Q. Chu, Structural Stability of Co Nanowire Arrays Embedded in the PAAM, *Phys. Lett. A*, 2006, **359**, 220.
- 23 B. W. Lee, R. Alsenz, A. Ignatiev, Surface Structures of the Two Allotropic Phases of Cobalt, *Phys. Rev. B*, 1978, **17**, 1510.
- 24 S. Jia, C.-H. Hsia, D. H. Son, In Situ Study of Room-Temperature Oxidation Kinetics of Colloidal Co Nanocrystals Investigated by Faraday Rotation Measurement, *J. Phys. Chem. C*, 2011, **115**, 92.
- 25 D. -H. Ha, L. M. Moreau, C. R. Bealing, H. Zhan, R. G. Hennig, R. D. Robinson, The Structural Evolution and Diffusion during the Chemical Transformation from Cobalt to Cobalt Phosphide Nanoparticles, *J. Mater. Chem.*, 2011, **21**, 11498.
- 26 K. Deori, S. Deka, Morphology Oriented Surfactant Dependent CoO and Reaction Time Dependent Co_3O_4 Nanocrystals from Single Synthesis Method and Their Optical and Magnetic properties, *CrystEngComm*, 2013, **15**, 8465.
- 27 B. D. Yuhas, D. O. Zitoun, P. J. Pauzauskie, R. He, P. Yang, Transition-Metal Doped Zinc Oxide Nanowires, *Angew. Chem.*, 2006, **45**, 420.
- 28 M. Ohtake, O. Yabuhara, Y. Nukaga, M. Futamoto, Preparation of $\text{Co}(0001)_{\text{hcp}}$ and $(111)_{\text{fcc}}$ Films on Single-Crystal Oxide Substrates, *J. Phys.: Conf. Ser.*, 2011, **303**, 012016.
- 29 Y. Yoo, I. Yoon, H. Lee, J. Ahn, J. P. Ahn, B. Kim, Pattern-Selective Epitaxial Growth of Twin-Free Pd Nanowires from Supported Nanocrystal Seeds, *ACS Nano*, 2010, **4**, 2919.
- 30 R. Cao, R. Deng, J. Tang, S. Song, Y. Lei, H. Zhang, Cobalt and Nickel with Various Morphologies: Mineralizer-Assisted Synthesis, Formation Mechanism, and Magnetic Properties, *CrystEngComm*, 2011, **13**, 223.
- 31 D. -H. Ha, L. M. Moreau, S. Honrao, R. G. Hennig, R. D. Robinson, The Oxidation of Cobalt Nanoparticles into Kirkendall-Hollowed CoO and Co_3O_4 : The Diffusion Mechanisms and Atomic Structural Transformations, *J. Phys. Chem. C*, 2013, **117**, 14303.
- 32 M. Martin, U. Koops, N. Lakshmi, Reactivity of Solid Studied in situ XAS and XRD, *Solid State Ionics*, 2004, **172**, 357.
- 33 Z. Yang, I. Lisiecki, M. Walls, M. -P. Pileni, Nanocrystallinity and the Ordering of Nanoparticles in Two-Dimensional Superlattices: Controlled Formation of Either Core/Shell (Co/CoO) or Hollow CoO Nanocrystals, *ACS Nano*, 2013, **7**, 1342.
- 34 T. Li, S. Yang, L. Huang, B. Gu, Y. Du, A Novel Process from Cobalt Nanowire to Co_3O_4 Nanotube, *Nanotechnology*, 2004, **15**, 1479.

Table of Contents



Ferromagnetic single-crystalline Co nanowires (NWs) aligned in a vertical orientation are epitaxially grown on *m*-cut sapphire substrates by rapid and versatile chemical vapor deposition method. They were transformed into Co_3O_4 nanotubes by thermal annealing in dilute O_2 condition.